

# Chemical Exchange

Pramodh Vallurupalli

February 24, 2009

Workshop Series on NMR and Related Topics

February 16-20, 2009

TIFR Mumbai

# Contents

<b>1</b>	<b>Introduction</b>	<b>3</b>
<b>2</b>	<b>Stochastic picture of chemical exchange</b>	<b>5</b>
<b>3</b>	<b>Phenomenological Kinetic equations</b>	<b>6</b>
<b>4</b>	<b>Bloch-McConnell equations</b>	<b>7</b>
4.1	Slow exchange . . . . .	11
4.2	Fast exchange . . . . .	12
4.3	Dependence of $R_{ex}$ on $B_0$ . . . . .	13
<b>5</b>	<b>ZZ Exchange experiment to study slow processes</b>	<b>15</b>
<b>6</b>	<b>Relaxation dispersion experiments for micro-millisecond time scale exchange</b>	<b>17</b>
6.1	CPMG experiments . . . . .	18
6.2	Determining the sign on $\Delta\varpi$ . . . . .	22
6.3	$R_{1\rho}$ experiments . . . . .	24
<b>7</b>	<b>Studying the pico-nanosecond timescale local flexibility in the presence of chemical exchange</b>	<b>27</b>
7.1	$^1\text{H}$ - $^{15}\text{N}$ Dipole-CSA cross-correlated measurement as a means of measuring the ground state $J(0)$ . . . . .	28
7.2	Linear combinations of $^1\text{H}$ and $^{15}\text{N}$ SQ and MQ relaxation rates to measure ground state $J(0)$ . . . . .	29
<b>8</b>	<b>References</b>	<b>30</b>

# 1 Introduction

The chemical shift of a nucleus is extremely sensitive to the surrounding chemical environment. Hence the chemical shift of a nucleus changes when the chemical environment around it changes. In a molecule this can occur either due to a chemical reaction or due to conformational changes (isomerization reactions). During these processes the nuclei are exchanging between different chemical environments which leads to this phenomena being called "chemical exchange" in the NMR literature. As solution NMR usually records the chemical shifts of the various nuclei in a molecule, chemical exchange affects the solution NMR spectrum of the molecule. Consider the case of the azapropzaone derivative shown in figure 1.

Rotation about the C-N bond can interconvert the positions of the two methyl groups which have different chemical environments.

At very low temperatures (223K bottom of figure 1) when this interconversion is nonexistent the  $^1\text{H}$  spectrum of the N-methyl groups consists of two sharp peaks arising from each of the methyl groups. As the temperature is increased and the rate of interconversion becomes faster, the peaks first broaden, then merge

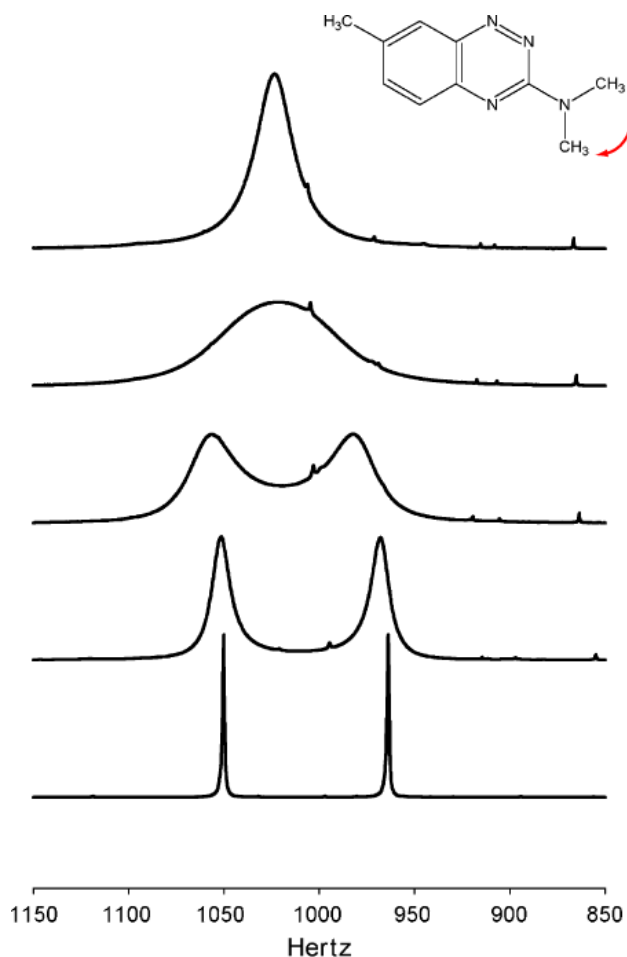


**Figure 1:** The N-methyl region from a 300 MHz  $^1\text{H}$  NMR spectrum of a azapropzaone derivate recorded at 223 (lowest), 243, 253, 263 and 273 (top) K. The figure is adapted from [Bain, 2003].

into a single broad peak and finally give rise to a narrow peak at the average position (of the two peaks). This sensitivity of the NMR spectrum to chemical exchange makes NMR a very powerful method to follow the kinetics and study the dynamics of molecules in solution.

A particularly impressive example of the use of NMR to characterize dynamics in solution is the study of the isomerization between the two boat forms of cyclohexane. Hasha, Eguchi, and Jonas [Hasha et al., 1982] monitored the effect of pressure on the isomerization reaction by NMR. Interestingly they found that initially the rate of interconversion increases with pressure although the volume of the transition state is slightly larger than the two boat forms. Contrary to popular belief which assumed that condensed phase reactions lie in the diffusive regime of the Kramer's model, this showed that the reaction lies in the inertial regime of the Kramer's model although it occurs in solution.

The initial studies of chemical exchange were confined to small molecules. However due to significant developments in NMR methodology over the last ten years, it is now possible to study conformational exchange in large macromolecules like proteins and to detect excited states which are transiently populated for short amounts of time, even though these cannot be observed in conventional NMR spectra. The aim of this set of lectures is to look at how chemical exchange affects NMR spectra and how we can derive information about the kinetics from the NMR spectra. Kinetic equations are revised in section 3. Section 4 introduces the Bloch-McConnell equations, using which we can calculate NMR spectra in the presence of chemical exchange. ZZ exchange experiments to study exchange in the second time scale is discussed in section 5. CPMG and  $R_{1,\rho}$  experiments are discussed in section 6. Section 7 differs from the others, rather than study chemical exchange, experiments to characterize pico-nanosecond timescale dynamics in the presence of chemical exchange are discussed. These lecture notes are quite concise. Please refer to the book Protein NMR Spectroscopy: Principles and Practice [Cavanagh et al., 2006] and the review article [Palmer et al., 2001] for a more detailed discussion of the subject.

## 2 Stochastic picture of chemical exchange

We start by considering the simple isomerization reaction:



Here  $k_1$  and  $k_{-1}$  are the first order forward and reverse rate constants. We are interested in the NMR spectrum of a nucleus in the molecule whose chemical shift is  $\omega_A$  in state A and  $\omega_B$  in state B, with  $\Delta\omega = \omega_B - \omega_A$ . Here  $\omega$  has units of radians/second and depends on the field strength while  $\varpi$  has units of ppm and is field independent. As the molecules are randomly jumping between the two states, the Hamiltonian is time dependent with the frequency at which the system evolves depending on the state the system is in:

$$\omega(t) = \omega_A + \Delta\omega h(t) \quad (2)$$

$$h(t) = \begin{cases} 0 & \text{state A} \\ 1 & \text{state B} \end{cases}$$

The observed signal  $\hat{M}^+ = \hat{M}_x + i\hat{M}_y$  is given by

$$\hat{M}^+(t) = \langle e^{i \int_0^t \omega(t) dt} \rangle \quad (3)$$

The outer average  $\langle \dots \rangle$  is over all the molecules in the sample. The integral is over a single molecule. It is not practical to solve this equation in most cases. Rather than solve it in specialized cases we will take the approach we do to study kinetics, where we use rate equations.

### 3 Phenomenological Kinetic equations

We can start by considering the simple isomerization reaction, equation (1). The concentrations of A and B are related to the rate constants by the following equations:

$$\begin{aligned}\frac{d[A]}{dt} &= -k_1[A] + k_{-1}[B] \\ \frac{d[B]}{dt} &= k_1[A] - k_{-1}[B]\end{aligned}\tag{4}$$

The rate equations can be rewritten in a matrix form as:

$$\frac{d}{dt} \begin{bmatrix} [A] \\ [B] \end{bmatrix} = \begin{bmatrix} -k_1 & k_{-1} \\ k_1 & -k_{-1} \end{bmatrix} \begin{bmatrix} [A] \\ [B] \end{bmatrix}\tag{5}$$

At equilibrium we have:

$$\frac{d[A]}{dt} = \frac{d[B]}{dt} = 0 \Rightarrow k_1[A_{eq}] - k_{-1}[B_{eq}] = 0 \Rightarrow \frac{[B_{eq}]}{[A_{eq}]} = \frac{k_1}{k_{-1}}\tag{6}$$

The fractional population in state B at equilibrium  $p_b = \frac{[B_{eq}]}{[A_{eq}] + [B_{eq}]} = \frac{k_1}{k_1 + k_{-1}}$  with  $p_b + p_a = 1$ .

We can solve the differential equations (3) to see how the system returns to equilibrium.

$\Delta A(t) = ([A] - [A_{eq}])$  is the deviation of the concentration of A from its equilibrium value.

We have

$$\Delta A(t) = \Delta A(0)e^{-k_{ex}t}\tag{7}$$

Here  $k_{ex} = k_1 + k_{-1}$ . The system returns to equilibrium with single rate constant  $k_{ex}$  and is characterized by a single timescale  $\tau_{ex} = 1/k_{ex}$ . Chemical exchange is discussed in terms of  $k_{ex}$  (the rate at which the system returns to equilibrium) and the fraction in the minor state  $p_b$ . Thus  $k_{ex}$  provides information regarding the kinetics of the processes while  $p_b$  provides information regarding the thermodynamics of the processes.

## Problems

1. For the two state reaction (1) show that  $k_{ex}$  and  $p_b$  are related to  $k_1$  and  $k_{-1}$  with  $k_1 = p_b k_{ex}$  and  $k_{-1} = p_a k_{ex} = (1 - p_b) k_{ex}$ .
2. Setup and solve the equations for a linear three state system  $A \xrightleftharpoons[k_{-1}]{k_1} B \xrightleftharpoons[k_{-2}]{k_2} C$ . How many timescales are involved?

## 4 Bloch-McConnell equations

The Bloch equation for evolution of magnetization in the presence of a  $B_0$  field in the  $z$  direction has the following form:

$$\frac{d}{dt} \begin{bmatrix} \hat{E} \\ \hat{M}_z \\ \hat{M}^+ \\ \hat{M}^- \end{bmatrix} = \begin{bmatrix} & & & \\ R_1 \hat{M}_{z0} & -R_1 & & \\ & & i\omega - R_2 & \\ & & & -i\omega - R_2 \end{bmatrix} \begin{bmatrix} \hat{E} \\ \hat{M}_z \\ \hat{M}^+ \\ \hat{M}^- \end{bmatrix} \quad (8)$$

where  $\hat{E}$  is the identity operator and  $R_1$  and  $R_2$  are the rates at which the longitudinal and transverse magnetization return to equilibrium.  $\hat{M}_{z0}$  is the equilibrium magnetization along the magnetic field ( $z$  axis). As we wish to calculate the lineshape observed after a pulse we can focus on only the transverse magnetization component  $\hat{M}^+ = \hat{M}_x + i\hat{M}_y$ . If we have two species A and B, the Bloch equations in the absence of chemical exchange for free precession of transverse magnetization is:

$$\frac{d}{dt} \begin{bmatrix} \hat{M}_A^+ \\ \hat{M}_B^+ \end{bmatrix} = \begin{bmatrix} -R_{2,A} + i\omega_A & \\ & -R_{2,B} + i\omega_B \end{bmatrix} \begin{bmatrix} \hat{M}^+ \\ \hat{M}^- \end{bmatrix} \quad (9)$$

Here  $\hat{M}_A^+$  and  $\hat{M}_B^+$  are the transverse magnetization components arising from species A and B respectively,  $\omega_A$  and  $\omega_B$  are the chemical shifts for species A and B while  $R_{2,A}$  and  $R_{2,B}$  are the transverse relaxation rates of species A and B. The total magnetization  $\hat{M}^+$  is the sum of the magnetization arising from each of the components,  $\hat{M}^+ = \hat{M}_A^+ + \hat{M}_B^+$ . Solving equation (9) gives:

$$\begin{bmatrix} \hat{M}_A^+(t) \\ \hat{M}_B^+(t) \end{bmatrix} = e^{\begin{bmatrix} -R_{2,A} + i\omega_A & \\ & -R_{2,B} + i\omega_B \end{bmatrix} t} \begin{bmatrix} \hat{M}_A^+(0) \\ \hat{M}_B^+(0) \end{bmatrix} \quad (10)$$

and leads to

$$\hat{M}^+(t) = \hat{M}_A^+(0)e^{(-R_{2,A}+i\omega_A)t} + \hat{M}_B^+(0)e^{(-R_{2,B}+i\omega_B)t} \quad (11)$$

The fourier transform of this signal gives the spectrum. As expected the imaginary part gives rise to two peaks at  $\omega_A$  and  $\omega_B$  with linewidths determined by the real part to be  $R_{2,A}$  and  $R_{2,B}$ . The volumes of the peaks are proportional to  $\hat{M}_A^+(0)$  and  $\hat{M}_B^+(0)$ . If a  $90^\circ$  pulse was applied at  $t = 0^-$  to the system at equilibrium then  $\hat{M}_A^+(0)$  and  $\hat{M}_B^+(0)$  are proportional to the concentrations of the two species  $p_a$  and  $p_b$ .

We consider the case when A and B interconvert  $A \xrightleftharpoons[k_{-1}]{k_1} B$ . Noting the similarity between concentrations and magnetization, we can introduce chemical exchange into the Bloch equations because the kinetic rate equations (5) have the same form as the Bloch equations (9).

$$\frac{d}{dt} \begin{bmatrix} \hat{M}_A^+ \\ \hat{M}_B^+ \end{bmatrix} = \left\{ \begin{bmatrix} -R_{2,A} + i\omega_A & \\ & -R_{2,B} + i\omega_B \end{bmatrix} + \begin{bmatrix} -k_1 & k_{-1} \\ k_1 & -k_{-1} \end{bmatrix} \right\} \begin{bmatrix} \hat{M}_A^+ \\ \hat{M}_B^+ \end{bmatrix} \quad (12)$$

Which can be conveniently written as:

$$\frac{d\vec{M}}{dt} = [i\hat{\omega} - \hat{R} + \hat{k}]\vec{M} \quad (13)$$

The Bloch equations modified to include chemical exchange are called the Bloch-McConnell equations.  $\vec{M}$  is the complete basis set of operators required,  $\hat{R}$  is the relaxation matrix for the basis set operators,  $\hat{\omega}$  is the evolution matrix for the operators.  $\hat{k}$  is rate matrix.

For an isolated spin- $\frac{1}{2}$  nucleus  $\vec{M} = \begin{bmatrix} \hat{M}_A^+ \\ \hat{M}_B^+ \end{bmatrix}$ ,  $\hat{\omega} = \begin{bmatrix} \omega_A & \\ & \omega_B \end{bmatrix}$ ,  $\hat{R} = \begin{bmatrix} R_{2,A} & \\ & R_{2,B} \end{bmatrix}$  and  $\hat{k} = \begin{bmatrix} -k_1 & k_{-1} \\ k_1 & -k_{-1} \end{bmatrix}$ . The Bloch-McConnell equations can be solved easily:

$$\vec{M}(t) = e^{[i\hat{\omega} - \hat{R} + \hat{k}]t} \vec{M}(0) \quad (14)$$

The solutions to (12) are given by:

$$\begin{bmatrix} \hat{M}_A^+(t) \\ \hat{M}_B^+(t) \end{bmatrix} = \begin{bmatrix} a_{11}(t) & a_{12}(t) \\ a_{21}(t) & a_{22}(t) \end{bmatrix} \begin{bmatrix} \hat{M}_A^+(0) \\ \hat{M}_B^+(0) \end{bmatrix} \quad (15)$$

with

$$\begin{aligned} a_{11} &= \frac{1}{2} \left[ \left( 1 - \frac{i\Delta\omega - \Delta R_2 + k_1 - k_{-1}}{(\lambda_+ - \lambda_-)} \right) e^{-\lambda_- t} + \left( 1 + \frac{i\Delta\omega - \Delta R_2 + k_1 - k_{-1}}{(\lambda_+ - \lambda_-)} \right) e^{-\lambda_+ t} \right] \\ a_{22} &= \frac{1}{2} \left[ \left( 1 + \frac{i\Delta\omega - \Delta R_2 + k_1 - k_{-1}}{(\lambda_+ - \lambda_-)} \right) e^{-\lambda_- t} + \left( 1 - \frac{i\Delta\omega - \Delta R_2 + k_1 - k_{-1}}{(\lambda_+ - \lambda_-)} \right) e^{-\lambda_+ t} \right] \\ a_{12} &= \frac{k_{-1}}{(\lambda_+ - \lambda_-)} [e^{-\lambda_- t} - e^{-\lambda_+ t}] \\ a_{21} &= \frac{k_1}{(\lambda_+ - \lambda_-)} [e^{-\lambda_- t} - e^{-\lambda_+ t}] \end{aligned}$$

where  $\Delta\omega = \omega_B - \omega_A$  and  $\Delta R_2 = R_{2,B} - R_{2,A}$  and the eigenvalues of the Bloch-McConnell

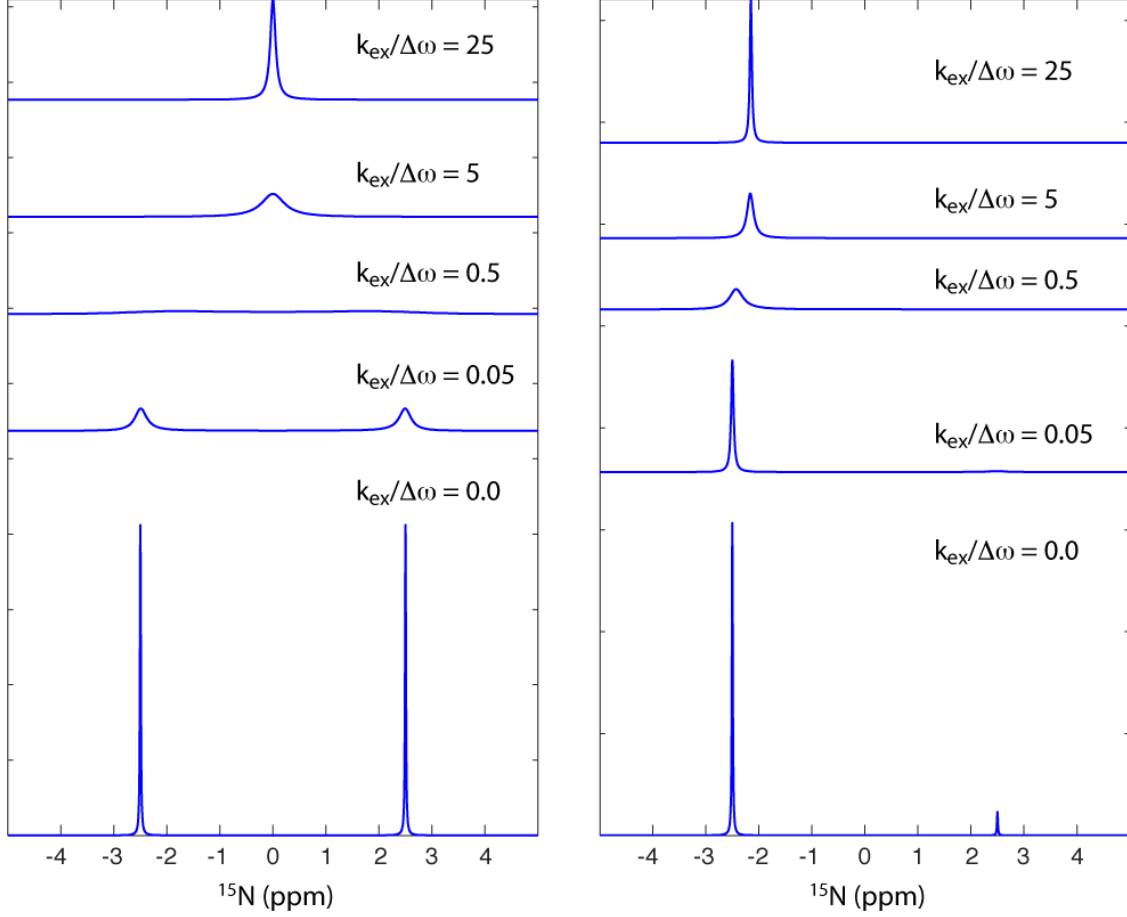


**Figure 2:** Spectra of  $^{15}\text{N}$  nucleus undergoing chemical exchange in a 800 MHz magnet, simulated using the Bloch-McConnell equations (12).  $\Delta\varpi = 5\text{ppm}$  and  $p_b = 0.5$  on the left and  $p_b = 0.07$  on the right

matrix  $\lambda_+$  and  $\lambda_-$  are given by

$$\lambda_{\pm} = \frac{1}{2} \left[ (-i\omega_A - i\omega_B + R_{2,A} + R_{2,B} + k_{ex}) \pm \left\{ (i\Delta\omega - \Delta R_2 + k_1 - k_{-1})^2 + 4k_1k_{-1} \right\}^{1/2} \right]$$

Spectra can be calculated (figure 2) using the Bloch-McConnell equations (12). In the case when the populations of the two states are equal ( $p_a = p_b = 0.5$ ) (figure 2 left) we find that when exchange is slow we have two peaks which broaden as the exchange rate increases and then merge into a single very wide peak as  $k_{ex} \sim \Delta\omega$  and finally we get a sharp peak at

the average position when  $k_{ex} \gg \Delta\omega$ . The more interesting case however is when one state ( $A$  here) has a higher population than the other state ( $p_a > p_b$ ). The case when  $p_a = 0.93$  and  $p_b = 0.07$  is shown on the right hand side of figure 2. When exchange is slow we have two peaks at  $\omega_A$  and  $\omega_B$  where the heights are proportional to the populations. However when the rate of exchange begins to increase we find that the minor peak broadens much more than the major peak and cannot be detected (This is discussed further in 4.1). The major peak on the other hand can be seen even if the minor peak cannot and initially continues to broaden as  $k_{ex}$  increases and then begins to become sharper as  $k_{ex}$  further increases. Finally when exchange is very fast we have a single peak at the average position. The exact positions and linewidths of the peaks can be obtained from the imaginary and real parts of eigenvalues of the matrix in equation (12).

## 4.1 Slow exchange

Without any loss of generality we can set  $\omega_A = 0$  in (12) which leads to  $\omega_B = \Delta\omega = \omega_B - \omega_A$ .  $\Delta\omega$  is the difference in the chemical shift of the coherences of interest between state B and state A. The Bloch-McConnell (12) equation now simplifies to:

$$\frac{d}{dt} \begin{bmatrix} \hat{M}_A^+ \\ \hat{M}_B^+ \end{bmatrix} = \begin{bmatrix} -R_{2,A} - k_1 & k_{-1} \\ k_1 & -R_{2,B} + i\Delta\omega - k_{-1} \end{bmatrix} \begin{bmatrix} \hat{M}_A^+ \\ \hat{M}_B^+ \end{bmatrix} \quad (16)$$

We can now look at the slow exchange limiting case when  $k_{ex} \ll |i\Delta\omega + \Delta R_2|$ , remembering that  $k_{ex} = k_1 + k_{-1}$  we can ignore the offdiagonal terms of the matrix in equation (16) as they are very small compared to the diagonal terms. This simplifies equation (16) to:

$$\frac{d}{dt} \begin{bmatrix} \hat{M}_A^+ \\ \hat{M}_B^+ \end{bmatrix} = \begin{bmatrix} -R_{2,A} - k_1 & \\ & -R_{2,B} + i\Delta\omega - k_{-1} \end{bmatrix} \begin{bmatrix} \hat{M}_A^+ \\ \hat{M}_B^+ \end{bmatrix} \quad (17)$$

which can be solved trivially to obtain:

$$\hat{M}^+(t) = \hat{M}_A^+(0)e^{(-R_{2,A}-k_1)t} + \hat{M}_B^+(0)e^{(-R_{2,B}+i\Delta\omega-k_{-1})t} \quad (18)$$

We once again have two peaks at  $\omega_A$  and  $\omega_B$  but the linewidths are no longer determined by just  $R_{2,A}$  and  $R_{2,B}$ . We can see that chemical exchange broadens the peaks and their linewidths are determined by  $R_{2,A} + k_1$  and  $R_{2,B} + k_{-1}$  for peak A and peak B respectively. The increase in the relaxation rate due to chemical exchange is called  $R_{ex}$ . In fact the two peaks are broadened differently due to chemical exchange with  $R_{ex,A} = k_1$  and  $R_{ex,B} = k_{-1}$ . This can be seen in figure 2 where the minor state B is broadened significantly more than the major state A. This occurs because once a molecule jumps from state A to B, it spends a lot of time in the new state, B and when it jumps back to A it has lost phase with the molecules in state A. Hence exchange gives rise to leaking effect and the rate loss of magnetization from A is determined by  $k_1$  and from B by  $k_{-1}$ . Now if B is the minor state  $k_{-1} > k_1$  which means the molecules spend less time in state B giving rise to very broad peaks in the minor state. The important consequence of this is that it is very difficult to observe the minor states in spectra even in slow exchange. Further a major peak that is not severely exchange broadened in the absence of minor peak does not mean fast exchange.

## 4.2 Fast exchange

In the fast exchange limit  $k_{ex} \gg \Delta\omega$  equation (15) reduce to

$$\hat{M}^+(t) = \hat{M}^+(0)e^{-(i\bar{\omega} + \bar{R}_2 + p_a p_b \Delta\omega^2 / k_{ex})t} \quad (19)$$

Here  $\bar{\omega} = p_a \omega_a + p_b \omega_b$  and  $\bar{R}_2 = p_a R_{2,a} + p_b R_{2,b}$  are the population weighted chemical shift and transverse relaxation rate. Here we have one peak at the average chemical shift.

This is because the molecules are interconverting rapidly between states A and B and so the magnetization arising from all the individual molecules is not dephasing significantly and evolving with the average chemical shift. There is some amount of dephasing because  $k_{ex} \neq \infty$ , which is reflected by  $R_{ex} = p_a p_b \Delta\omega^2 / k_{ex}$ .

### 4.3 Dependence of $R_{ex}$ on $B_0$

We will now look at how the exchange contribution to relaxation ( $R_{ex}$ ) depends on the field strength. This arises because because  $\Delta\omega \propto B_0$ . We will focus on the major peak A assuming  $p_a > p_b$ . In the slow exchange limit (section 4.1) the linewidth of the major peak depends only on  $k_1$  and not on the field strength  $B_0$ . In the fast exchange limit however the  $R_{ex} \propto B_0^2$  (equation (19)). The parameter  $\alpha$  relates  $R_{ex}$  to  $B_0$ .  $\alpha$  is defined as [Palmer et al., 2001]:

$$\begin{aligned} \frac{\delta R_{ex}}{R_{ex}} &= \alpha \frac{\delta B_0}{B_0} \\ \frac{d \ln R_{ex}}{d \ln \Delta\omega} &= \alpha \end{aligned} \tag{20}$$

When  $p_a > 0.7$  and  $R_{2,A} = R_{2,B}$  it can be shown that:

$$R_{ex} = \frac{p_a p_b k_{ex}}{1 + (k_{ex}/\Delta\omega)^2} \tag{21}$$

which leads to the following relations between  $\alpha$  and the regimes of exchange:

$$\begin{aligned} 0 &\leq \alpha < 1 && \text{slow exchange} \\ \alpha &= 1 && \text{intermediate exchange} \\ 1 &< \alpha \leq 2 && \text{fast exchange} \end{aligned} \tag{22}$$

The above discussion tells us that the linewidth of the major state peak does not depend on the field strength when we are in the slow exchange limit and increases quadratically with field strength in the fast exchange limit as can be seen from equations (18) and (19) also. In a protein which is undergoing a single conformational exchange processes this tells us that peaks with low  $\Delta\varpi$  will broaden due to chemical exchange when the field strength is increased but peaks with large  $\Delta\varpi$  will not be affected (if they are in slow exchange).

We can now move to looking at the linewidth as a function of  $\Delta\omega$  for a given set of kinetic parameters ( $p_a, k_{ex}$  etc). In the slow and fast exchange limits for the major state peak  $A$  we have:

$$\begin{aligned} R_{ex} &= p_b k_{ex} \quad k_{ex}/\Delta\omega \rightarrow 0 \quad \text{slow exchange} \\ R_{ex} &= \frac{p_a p_b \Delta\omega^2}{k_{ex}} \quad k_{ex}/\Delta\omega \rightarrow \infty \quad \text{fast exchange} \end{aligned} \tag{23}$$

$R_{ex}$  in the slow exchange limit is  $k_1$  and is greater than the fast exchange values which tends to zero. As discussed earlier in the slow exchange limit, exchange leads to only a loss of magnetization and so for a given set of kinetic parameters ( $k_{ex}$  and  $p_b$ )  $R_{ex}$  is higher when  $\Delta\omega$  is higher. This means that as we go to higher field strengths exchange will lead to greater broadening of peaks approaching the slow exchange limit  $R_{ex} = p_b k_{ex}$ .

## Problems

1. Setup the complete Bloch-McConnell equations for a single spin exchanging between two states  $A \xrightleftharpoons[k_{-1}]{k_1} B$ . You will have to use four basis operators  $\hat{E}$ ,  $\hat{M}_z$ ,  $\hat{M}^+$  and  $\hat{M}^-$ . How big are the matrices?
2. How big will the matrices be if we have a two spin system exchanging between two states  $A \xrightleftharpoons[k_{-1}]{k_1} B$ ?
3. Numerically solve the transverse Bloch-McConnell equations (16), in a program like MATLAB and make sure that you can generate the curves in figure 2.

4. Numerically solve the transverse Bloch-McConnell equations (16) to obtain a  $R_{ex}$  vs  $\Delta\omega$  curve for  $p_b = 0.1$  and  $k_{ex} = 1000 \text{ s}^{-1}$ . When and what are highest and lowest  $R_{ex}$  values.

## 5 ZZ Exchange experiment to study slow processes

The ZZ exchange experiment is used to characterize slow conformational exchange processes in proteins when  $k_{ex}$  lies between 0.1 to 10  $\text{s}^{-1}$ . These experiments work by monitoring the exchange of longitudinal magnetization between the major and minor peaks as a function of time. As  $k_{ex}$  is slow the minor peak is not significantly broadened but it should be visible which means  $p_b \geq 0.1$ . The longitudinal Bloch-McConnell equations are:

$$\frac{d}{dt} \begin{bmatrix} \Delta \hat{M}_{z,A} \\ \Delta \hat{M}_{z,B} \end{bmatrix} = \left\{ \begin{bmatrix} -R_{1,A} & \\ & -R_{1,B} \end{bmatrix} + \begin{bmatrix} -k_1 & k_{-1} \\ k_1 & -k_{-1} \end{bmatrix} \right\} \begin{bmatrix} \Delta \hat{M}_{z,A} \\ \Delta \hat{M}_{z,B} \end{bmatrix} \quad (24)$$

Here  $\Delta \hat{M}_{z,A} = \hat{M}_{z,A} - \hat{M}_{0,z,A}$  where  $\hat{M}_{0,z,A}$  is the equilibrium z magnetization for state A. Equation (24) can be solved to obtain:

$$\begin{bmatrix} \Delta \hat{M}_{z,A}(t) \\ \Delta \hat{M}_{z,B}(t) \end{bmatrix} = \begin{bmatrix} a_{11}(t) & a_{12}(t) \\ a_{21}(t) & a_{22}(t) \end{bmatrix} \begin{bmatrix} \Delta \hat{M}_{z,A}(0) \\ \Delta \hat{M}_{z,B}(0) \end{bmatrix} \quad (25)$$

Magnetization transfer occurs only when the magnetization is out of equilibrium. When  $R_{1,A} = R_{1,B} = R_1$  we have:

$$\begin{aligned} a_{11} &= [p_a + p_b e^{-2k_{ex}t}] e^{-R_1 t} \\ a_{22} &= [p_b + p_a e^{-2k_{ex}t}] e^{-R_1 t} \\ a_{12} &= p_a [1 - e^{-2k_{ex}t}] e^{-R_1 t} \\ a_{21} &= p_b [1 - e^{-2k_{ex}t}] e^{-R_1 t} \end{aligned} \quad (26)$$

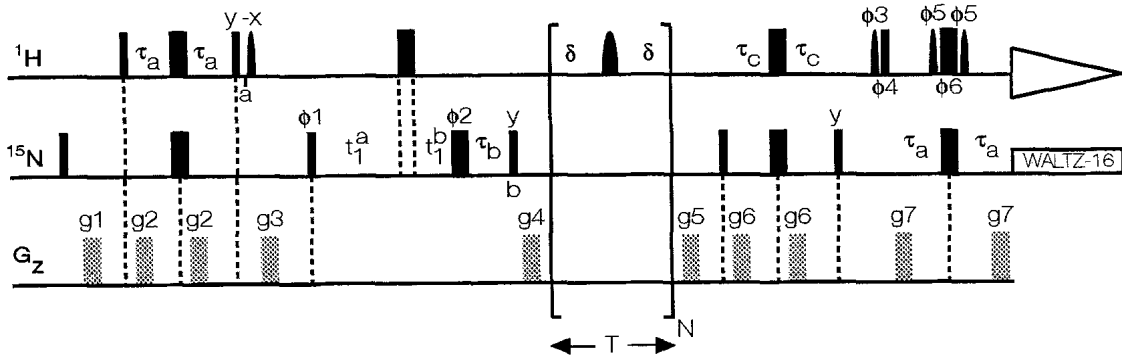


**Figure 3:** Pulse sequence for the ZZ exchange experiment to study slow conformational exchange in proteins at the  $^{15}\text{N}$ - $^1\text{H}$  backbone amide groups. More details can be found in the paper by Farrow, Zhang, Forman-Kay, and Kay [Farrow et al., 1994].

The pulse sequence for the ZZ exchange experiment to study chemical exchange at the backbone amide  $^{15}\text{N}$ - $^1\text{H}$  groups in proteins is shown in figure 3. Magnetization starting on the amide proton is transferred to nitrogen where it is labeled with the  $^{15}\text{N}$  chemical shift during  $t_1$  and then converted to  $N_z$  type magnetization. Now we have nonequilibrium  $^{15}\text{N}$  magnetization along the Z axis. This leads to magnetization transfer between states  $A$  and  $B$  during the mixing time  $T$ . Magnetization is then transferred back to the proton for detection. Four peaks, the two autopeaks  $(\omega_{N,A}, \omega_{H,A})$  and  $(\omega_{N,B}, \omega_{H,B})$  and the two crosspeaks due to magnetization transfer during  $T$   $(\omega_{N,B}, \omega_{H,A})$  and  $(\omega_{N,A}, \omega_{H,B})$  are observed in the 2D spectrum (figure 4). The intensities of the auto peaks evolve as  $a_{11}$  and  $a_{22}$  while the intensities of the crosspeaks evolve as  $a_{12}$  and  $a_{21}$  (figure 4).  $k_{ex}$  can be obtained from the volumes of the peaks in spectra recorded with different mixing times (figure 4). The populations of the two states are obtained from the volumes of the peaks which necessitates that the magnetization has fully relaxed before each transient. As this may not be practical the populations can be obtained from a simple 2D HSQC obtained with a long recycle delay. Sometimes it might be necessary to numerically account for the losses of magnetization during transfer periods.

The ZZ experiment can be used only when the major and minor state peaks are well

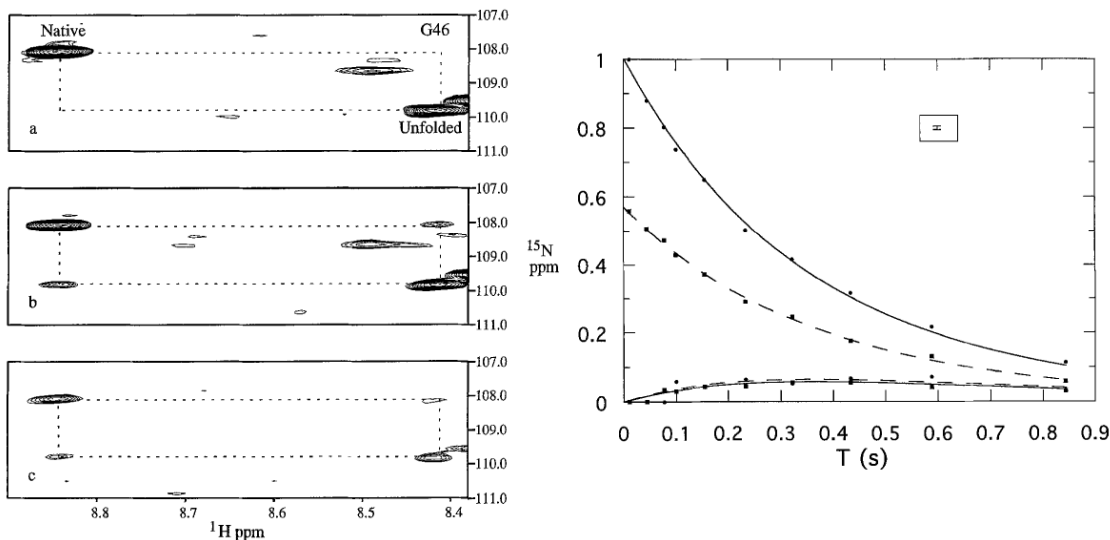


**Figure 4:** Folding-Unfolding of the Drk-SH3 domain studied using ZZ exchange experiment at  $14^{\circ}\text{C}$  [Farrow et al., 1994]. The crosspeak between the folded and unfolded state peaks becomes more intense compared to the autopeak as the mixing time  $T$  is increased from 0.11 to 0.843 s. The theoretical expressions are fitted to intensities of the peaks from the spectra to obtain  $k_{unfolding} = 0.43 \pm 0.03\text{s}^{-1}$  and  $k_{folding} = 0.86 \pm 0.06\text{s}^{-1}$ .

separated in both the dimensions and are both visible. The cross peaks will be less intense than the minor peak. Further only  $k_{ex} > R_1$  can be accurately determined because all magnetization will be lost if  $T$  is too long. In spite of these limitations this is very useful experiment which has been used to study protein folding and a version of the experiment performed using methyl groups has been used to characterize the opening and closing motion of the gates in the 300 kD ClpP protease.

## 6 Relaxation dispersion experiments for micro-millisecond time scale exchange

CPMG and  $R_{1\rho}$  experiments can be used to study exchange even when the minor state peak is not visible. Here state  $A$  will be the major state and  $B$  the minor state. In these experiments the kinetics of the exchange processes is characterized by studying the relaxation

properties of the state  $A$ .

## 6.1 CPMG experiments

In a CPMG experiment the relaxation properties of transverse magnetization is monitored after a series of  $\pi$  pulses. Transverse magnetization can be either due to single quantum (SQ) or multi quantum (MQ) transitions. In the constant time CPMG experiment the effective relaxation rate  $R_{2,eff}$  is monitored as function of the frequency ( $\nu_{CPMG}$ ) at which  $\pi$  pulses are applied during the constant time relaxation delay ( $T_{relax}$ ).  $N$   $\pi$  pulses are applied in  $\tau_{CPMG} - \pi - \tau_{CPMG}$  blocks such that  $2 \times N \times \tau_{CPMG} = T_{relax}$ . We also have:

$$\nu_{CPMG} = \frac{1}{4\tau_{CPMG}} \quad (27)$$

$$R_{2,eff} = \frac{-1}{T_{relax}} \ln \frac{I}{I_0} \quad (28)$$

Here  $I$  is the intensity of the peak in the spectrum and  $I_0$  is the intensity in a reference spectrum recorded without the relaxation delay  $T_{relax}$ . The lowest value of  $\nu_{CPMG}$  is determined by  $T_{relax}$  while the highest value is determined by the pulse handling capabilities of the probe. It is routinely possible to achieve  $\nu_{CPMG} = 1000$  Hz for  $^{15}\text{N}$ , 1500 Hz  $^{13}\text{C}$  and 2000 Hz for  $^1\text{H}$ . We can understand the idea behind the CPMG experiment by recognizing that the  $\pi$  pulses refocus chemical shift evolution. Thus applying a series of  $\pi$  pulses reduces the amount of chemical shift evolution. If the  $\pi$  pulses are applied at the appropriate speed this can move exchange from the slow to fast regime. Remembering that  $R_{ex}$  is highest when exchange is slow and  $R_{ex} = 0$  when exchange is fast,  $R_{2,eff}$  reduces with increasing  $\nu_{CPMG}$ . The effects of chemical exchange can be quenched only if  $\nu_{CPMG}$  is high enough.  $k_{ex}$  up to  $2000 \text{ s}^{-1}$  can be studied by carbon and nitrogen CPMG experiments and  $k_{ex}$  up to  $3000 \text{ s}^{-1}$  can be studied using proton CPMG experiments.  $k_{ex}$ ,  $p_b$  and  $|\Delta\omega|$  can be obtained by

analyzing the  $R_{2,eff}$  vs  $\nu_{CPMG}$  relaxation dispersion (RD) curve. To do this we have to be able to calculate effect of the CPMG sequence  $[\tau_{CPMG} - \pi - \tau_{CPMG}]_N$  on the transverse magnetization. We know how the magnetization evolves during the free precession periods. The  $\pi$  pulses effectively invert the sign of the precession. Normally  $N$  is even because having two  $\pi$  pulses compensates for pulse imperfections. Hence the effective evolution matrix  $\hat{U}_{CPMG}$  is:

$$\hat{U}_{CPMG} = [e^{\hat{R}(\Delta\omega)\tau_{CPMG}} e^{\hat{R}(-\Delta\omega)\tau_{CPMG}} e^{\hat{R}(-\Delta\omega)\tau_{CPMG}} e^{\hat{R}(\Delta\omega)\tau_{CPMG}}]^{\frac{N}{2}} \quad (29)$$

where  $\hat{R}(\Delta\omega)$  is the matrix in equation (16). The magnetization at the end of the CPMG sequence is given by

$$\begin{aligned} \vec{M} &= \hat{U}_{CPMG} \vec{M}(0) \\ \vec{M}(0) &= \begin{bmatrix} p_a \\ p_b \end{bmatrix} \end{aligned} \quad (30)$$

Using equation (30) one can calculate the effect of the CPMG sequence on the starting magnetization and compute the  $R_{2,eff}$  vs.  $\nu_{CPMG}$  curve for a given  $\Delta\varpi$ ,  $k_{ex}$ ,  $p_b$ ,  $R_{2,A}$  and  $R_{2,B}$ . Normally one assumes  $R_{2,A} = R_{2,B} = R_{2,\infty}$ . By numerical fitting to the experimental relaxation dispersion curve  $k_{ex}$ ,  $p_b$ ,  $|\Delta\varpi|$  can be obtained. Usually  $k_{ex}$ ,  $p_b$  and  $|\Delta\varpi|$  are correlated to some extent. Performing the experiments at two fields breaks this correlation because  $\Delta\omega$  scales according to the fields while the second field introduces only one new parameter ( $R_{2,\infty}$ ) at the new field. Further  $k_{ex}$  and  $p_b$  are fitted globally for all the peaks that are part of the same exchange processes.

Figure 5 shows a pulse sequence for recording  $^{15}\text{N}$  CPMG data for in  $^{15}\text{N}-^1\text{H}$  groups of proteins. Magnetization is transferred from  $^1\text{H}$  to  $^{15}\text{N}$  to generate inphase  $^{15}\text{N}$  magnetization. Refocusing pulses are applied on the inphase magnetization during the relaxation delay.  $^1\text{H}$  continuous wave (CW) decoupling is performed to keep the magnetization inphase wrt to  $^1\text{H}$ . Magnetization is then labeled with the nitrogen shift in the  $t_1$  dimension and transferred

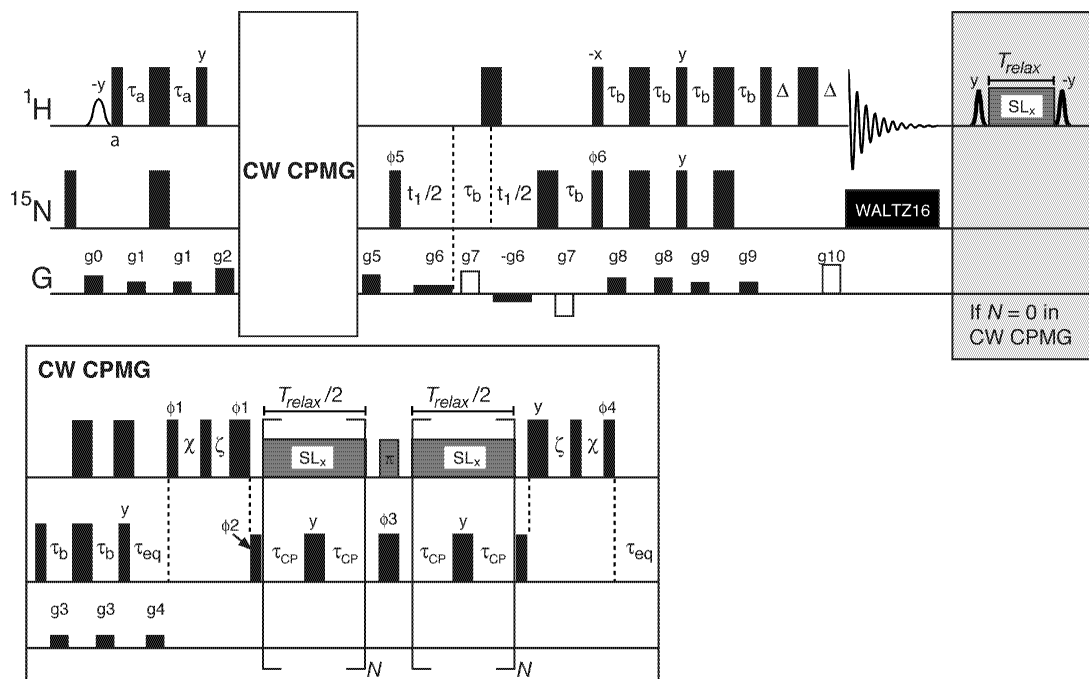


**Figure 5:**  $^{15}\text{N}$  CPMG pulse sequence to study chemical exchange at the backbone amides of proteins. The CPMG experiment is performed on the inphase  $^{15}\text{N}$  magnetization. Details can be found in [Hansen et al., 2008].

back to proton for detection to obtain conventional two dimensional  $^{15}\text{N}-^1\text{H}$  HSQC spectrum where the intensity of the peaks is quantified to obtain the Relaxation Dispersion curve.

Quantitative experiments like the CPMG experiments to quantify chemical exchange should be designed very carefully with systematic errors minimized. This is illustrated in the case of the TROSY CPMG experiment shown in figure 6. Here CPMG is performed on the  $^{15}\text{N}$  TROSY component  $N_x H^\beta$  which has better relaxation properties for large molecules. However  $^1\text{H}$  spin flips can interconvert the TROSY and Anti-TROSY ( $N_x H^\beta \rightleftharpoons N_x H^\alpha$ ) components leading to relaxation dispersion in the absence of exchange. The effect of this cross relaxation can be reduced by the P-Element [Loria et al., 1999] which inverts the TROSY component wrt to the Anti-TROSY component in middle of the sequence leading to a cancellation of the effects of cross-relaxation to first order. This can be seen easily in the

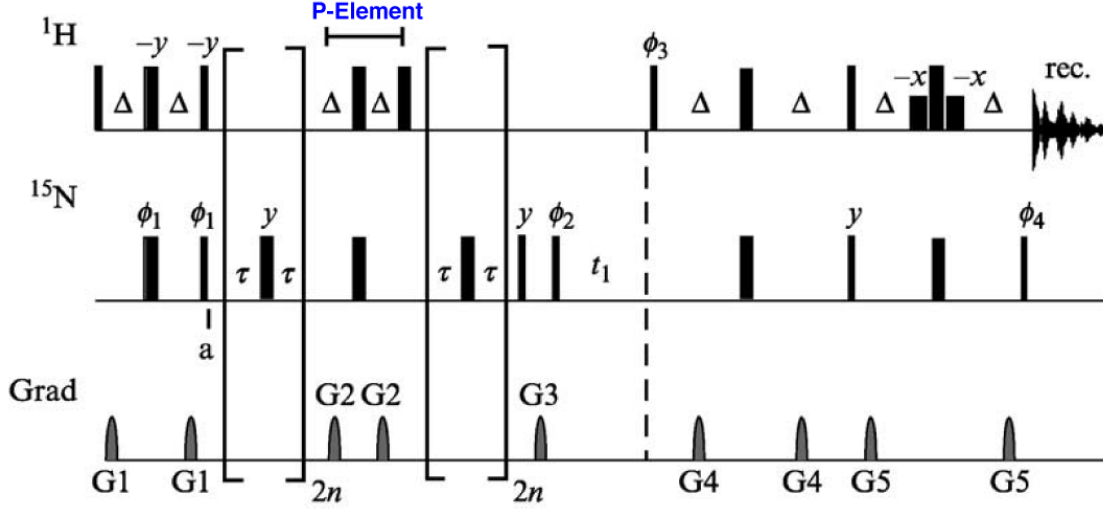


**Figure 6:**  $^{15}\text{N}$  TROSY CPMG pulse sequence to study chemical exchange at the backbone amides of proteins. The CPMG experiment is performed on the Trosy component  $^{15}\text{N}$  magnetization. The P-Element in the middle of the CPMG period reduces the effect of cross relaxation between the Trosy and Anti-Trosy components by inverting the Trosy component with respect to the Anti-Trosy component. Details can be found in [Loria et al., 1999].

absence of exchange by thinking of the subspace consisting of the TROSY and Anti-TROSY components only:

$$\begin{aligned}
\begin{bmatrix} \hat{M}_{TR}^+(T) \\ \hat{M}_{ATR}^+(T) \end{bmatrix} &= e^{\begin{bmatrix} -R_{TR} - i\pi j & \eta \\ \eta & -R_{ATR} + i\pi j \end{bmatrix} \frac{T}{2}} \begin{bmatrix} -1 \\ 1 \end{bmatrix} e^{\begin{bmatrix} -R_{TR} - i\pi j & \eta \\ \eta & -R_{ATR} + i\pi j \end{bmatrix} \frac{T}{2}} \begin{bmatrix} \hat{M}_{TR}^+(0) \\ \hat{M}_{ATR}^+(0) \end{bmatrix} \\
&= \begin{bmatrix} -1 \\ 1 \end{bmatrix} e^{\begin{bmatrix} -R_{TR} - i\pi j & -\eta \\ -\eta & -R_{ATR} + i\pi j \end{bmatrix} \frac{T}{2}} e^{\begin{bmatrix} -R_{TR} - i\pi j & \eta \\ \eta & -R_{ATR} + i\pi j \end{bmatrix} \frac{T}{2}} \begin{bmatrix} \hat{M}_{TR}^+(0) \\ \hat{M}_{ATR}^+(0) \end{bmatrix} \\
&\approx \begin{bmatrix} -1 \\ 1 \end{bmatrix} e^{\begin{bmatrix} -R_{TR} - i\pi j & \\ & -R_{ATR} + i\pi j \end{bmatrix} T} \begin{bmatrix} \hat{M}_{TR}^+(0) \\ \hat{M}_{ATR}^+(0) \end{bmatrix} \quad (31)
\end{aligned}$$

Here  $R_{TR}$  and  $R_{ATR}$  are the relaxation rates of the TROSY and Anti-TROSY components and  $\eta$  is cross-relaxation rate with  $\eta = \frac{1}{2}R_1(H)$ . The effect of the P element is taken into effect via  $\begin{bmatrix} -1 \\ 1 \end{bmatrix}$ , which eliminates the effects of  $\eta$  to first order. Figure 7 shows examples of relaxation dispersion curves.

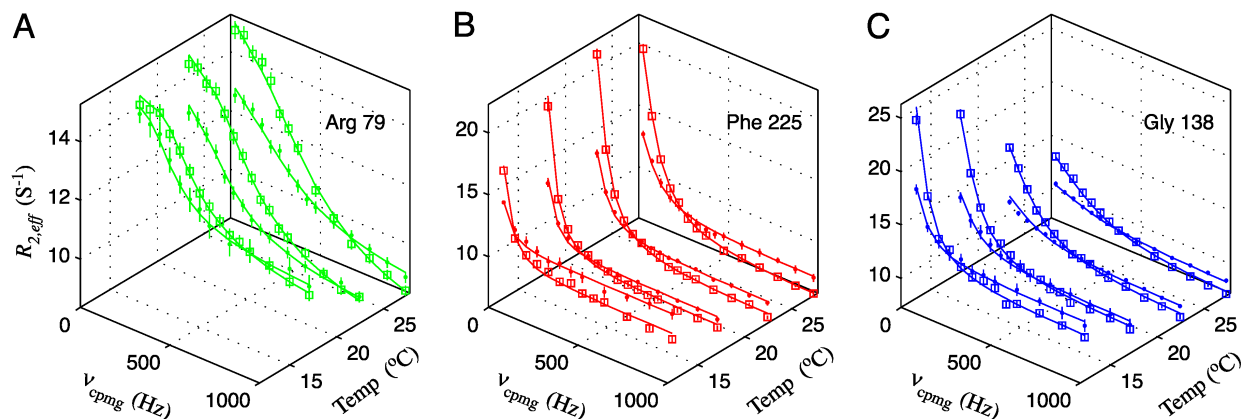


**Figure 7:**  $^{15}N$  TROSY relaxation dispersion profiles for Arg-79 (A), Phe-225 (B), and Gly-138 (C) from the protein flavin oxido-reductase recorded at magnetic field strengths of 11.7 ( $\bullet$ ) and 18.8 ( $\square$ ) T, as a function of temperature. The dispersions have different shapes and temperature dependencies showing that the protein is experiencing multiple dynamic processes in the millisecond timescale.

## Problems

1. Work out why even  $\pi$  pulses are better than an odd number of  $\pi$  pulses during a CPMG sequence. You can compare the effect of one and two pulses using vector diagrams.
2. The relative sign of the  $\Delta\omega$  of two nuclei can be obtained by comparing zero quantum (ZQ) and double (DQ) dispersions. Understand how this works by thinking about the frequencies involved in the case of a  $^{15}N-^1H$  spin system.

## 6.2 Determining the sign on $\Delta\varpi$

The CPMG experiments are insensitive to the sign of  $\Delta\varpi$ . The sign of  $\Delta\varpi$  is required to uniquely obtain the excited state chemical shift. The sign of  $^{15}\text{N}$   $\Delta\varpi$  can be obtained by comparing the positions of the peaks in  $^{15}\text{N}$ - $^1\text{H}$  HSQC spectra recorded at two field strengths. At lower fields the major state peak moves more towards the minor state peak. Comparing the positions of peaks in the indirect dimension of HSQC recorded at two fields gives the sign of the shift. Further we can also compare the positions of peaks in the indirect dimension of HSQC and HMQC spectra recorded at the same field. The peak positions differ in the two spectra because the HMQC peaks evolve as zero quantum (ZQ) for half the  $t_1$  and double quantum (DQ) for the other half.

These two coherence average nonlinearly to give rise to peaks that differ from their positions in the HSQC as long as  $\Delta\omega_H \neq 0$ . It turns out that for almost all  $p_b$  and  $k_{ex}$  values normally encountered, the major peak positions in the HSQC spectra are shifted slightly towards the minor peak compared to the HMQC spectra. This idea is illustrated in figure 8.

The  $^1\text{H}$  chemical shift is usually obtained by obtaining the relative sign of the shift from ZQ and DQ dispersions and using the carbon and nitrogen shift information that has been obtained.

## Problems

1. Derive expressions for the shift between the major state peak at two fields in HSQC spectra.

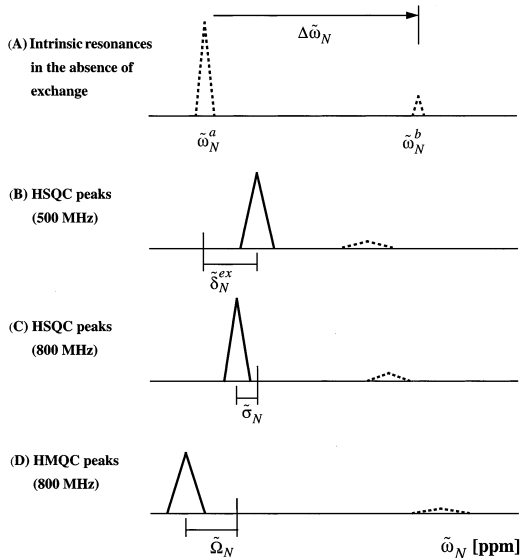


**Figure 8:** Schematic illustration of the peak positions in HSQC and HMQC spectra illustrating the idea behind obtaining the sign of  $\Delta\varpi$  by comparing major state peak positions in various spectra

2. Derive expressions for the shift between major state peaks in HSQC and HMQC recorded at the same field.

### 6.3 $R_{1\rho}$ experiments

$R_{1\rho}$  experiments are used to characterize exchange processes where  $k_{ex}$  can be in the range between 5,000 to 50,000  $s^{-1}$ . The exchange processes is characterized by measuring relaxation rates ( $R_{1\rho}$ ) when the magnetization is spin-locked using a RF field.

$$R_{1\rho} = R_1 \cos^2 \theta + R_2 \sin^2 \theta \quad (32)$$

with  $\tan \theta = \frac{\omega_1}{\Delta\Omega}$ , where  $\Delta\Omega = (p_a\omega_a + p_b\omega_b - \omega_{RF})$  is the offset of the population weighted chemical shift from the carrier frequency ( $\omega_{RF}$ ) and  $\omega_1$  is the field strength of the applied RF field. The effective field  $\omega_{eff} = \sqrt{\omega_1^2 + \Delta\Omega^2}$ .

$R_2$  can be obtained from  $R_{1\rho}$  after  $R_1$  has been measured.

The  $R_{ex}$  contribution to  $R_2$  is quenched by the applied RF field according to (in the fast exchange limit and when  $\omega_{eff}$  is the same for all the sites (A and B here)  $\omega_1 \gg \Delta\omega$ ):

$$R_{1\rho} = R_{1\rho(\omega_{eff} \rightarrow \infty)} + \sin^2 \theta \frac{p_a p_b \Delta\omega^2 k_{ex}}{k_{ex}^2 + \omega_{eff}^2} \quad (33)$$

When a strong RF field is applied on resonance  $\omega_{eff} = \omega_1$  then we can think of it as a series of  $\pi$  pulses like a CPMG experiment and increasing  $\omega_{eff}$  is the same as increasing  $\omega_1$  which corresponds to applying more closely spaced RF pulses which quenches  $R_{ex}$ . However  $\omega_{eff}$  can be increased by keeping  $\omega_1$  fixed and moving the carrier offresonance to quench

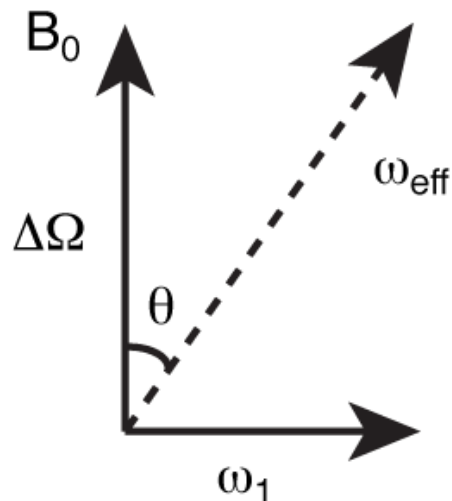


**Figure 9:** Effective field for  $R_{1\rho}$  measurements.

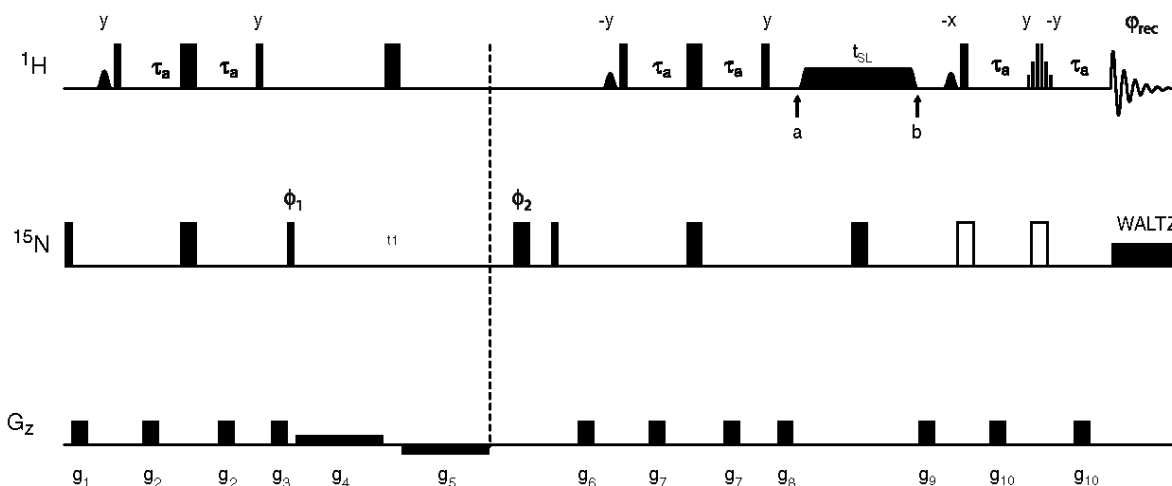


**Figure 10:**  $^1\text{H}$   $R_{1,\rho}$  experiment for characterizing  $\mu\text{s}$  time scale exchange in proteins at the amide position. Magnetization has to be aligned along the effective field to maximize sensitivity and this is done using variety of alignment schemes including adiabatic pulses. Details can be found in [Lundstrom and Akke, 2005]. This sequence was used to characterize exchange in a calmodulin mutant where  $k_{ex} \approx 50,000 \text{ s}^{-1}$ .

$R_{ex}$ . This can be understood from figure 9 as  $\Delta\Omega$  is increased  $\theta$  goes towards zero and the magnetization spends more time along the z axis where  $\Delta\omega = 0$  and so exchange is moved into the fast exchange regime quenching  $R_{ex}$ .

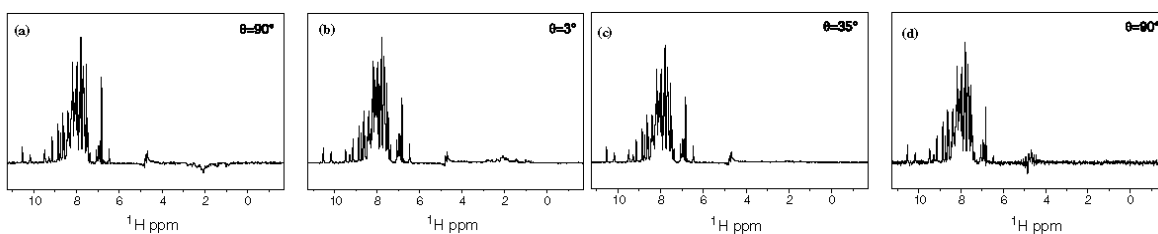


**Figure 11:** Amide-Aliphatic cross relaxation can be seen from the 1d traces of calmodulin recorded using the pulse sequence shown in figure 10 [Lundstrom and Akke, 2005]. In A the effects are due the ROE effect and in B they are due to the NOE effect and have the opposite sign. In C the two effects are of equal magnitude and cancel one another. In D cross relaxation is cancelled by inverting the aliphatic resonances selectively in the middle of the spinlock period.

The  $^1\text{H}$   $R_{1,\rho}$  experiments are particularly powerful to study fast chemical exchange as large  $\omega_{eff}$  fields can easily be applied due to the large  $^1\text{H}$   $\gamma$  values. The pulse sequence for

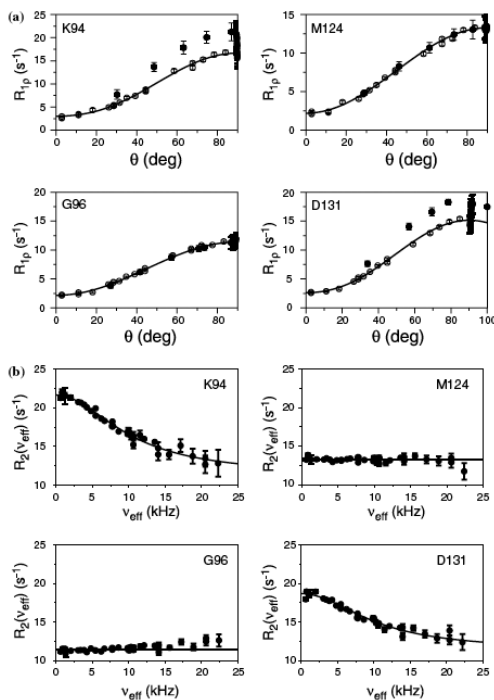


**Figure 12:**  $^1\text{H}$   $R_{1,\rho}$  and  $R_2$  dispersions recorded using the pulse sequence shown in figure 10.  $R_2$  has high errors at large  $\omega_{\text{eff}}$  as they are measured with small  $\theta$  when the  $R_2$  contribution to  $R_{1,\rho}$  is very small.

a  $^1\text{H}$   $R_{1,\rho}$  experiment is shown in figure 10. In this experiment cross relaxation (NOE and ROE) effects between the amide and aliphatic protons during the spin-lock (figure 11) can give rise to errors. This can be overcome by  $^2\text{H}$  enhancement of the protein to eliminate the aliphatic protons or by modifying the pulse sequence. Modifications include inverting only the aliphatic protons in the middle of the spin lock which inverts the sign of the cross relaxation term leading to a cancellation of the cross-relaxation effects. At low  $\theta$  values the NOE dominates cross relaxation while as  $\theta$  approaches  $90^\circ$  the ROE dominates cross relaxation. Hence a trick is to perform the experiments with  $\theta = 35^\circ$  as the NOE and ROE effects have equal and opposite signs at this angle leading to a cancellation of cross relaxation effects.

The above discussion is valid for strong  $\omega_1$  fields. However when small  $\omega_1$  fields are

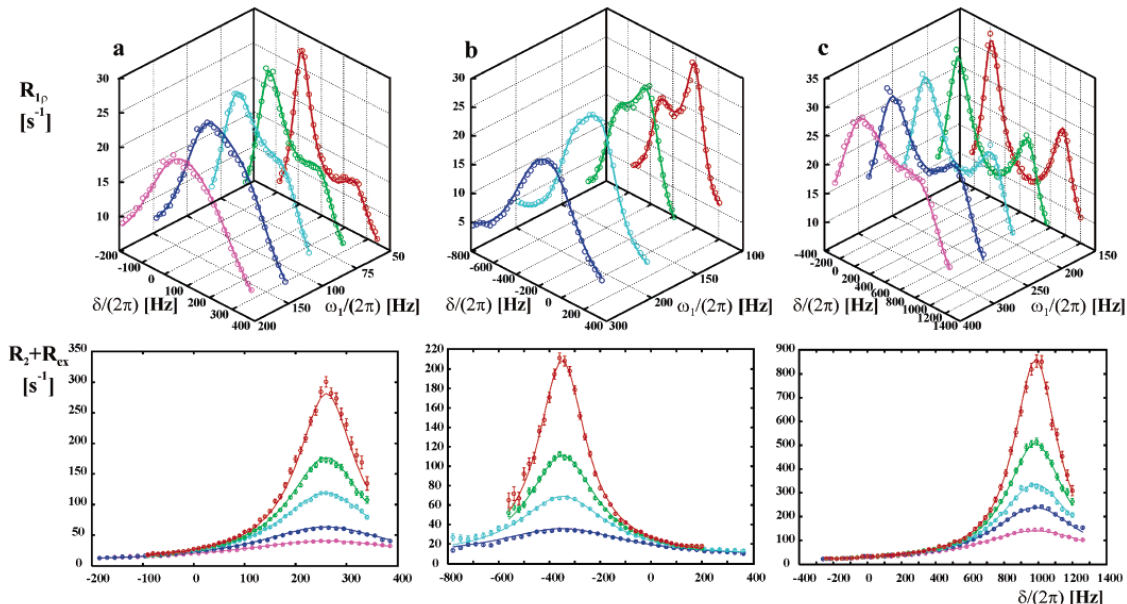


**Figure 13:**  $^{15}\text{N}$  off resonance  $R_{1\rho}$  and  $R_2$  profiles for three residues from Fyn SH3 G48M characterizing the folding-unfolding transition. The  $R_2$  profiles are extracted from the measured  $R_{1\rho}$  data. At low  $\omega_1$  fields two maxima are seen corresponding to the major and minor state peaks in the  $R_{1\rho}$  profile. The  $R_2$  profile is shifted towards the minor peak. See [Korzhnev et al., 2005] for the pulse sequence and more details.

applied,  $R_{1\rho}$  has a dependence on  $\omega_{rf}$  and  $\Delta\Omega$  which can give the sign of  $\Delta\Omega$ . This is illustrated in figure 13.

## 7 Studying the pico-nanosecond timescale local flexibility in the presence of chemical exchange

In proteins pico-nanosecond (ps-ns) timescale backbone dynamics is usually studied using  $^{15}\text{N}$   $R_1$ ,  $R_2$  and NOE experiments. The measured  $R_1$ ,  $R_2$  and NOE values can be interpreted in terms of local motion because they depend on the spectral density functions ( $J(\omega)$ ) where  $\omega$  takes values which are linear combinations of  $\omega_N$  and  $\omega_H$ . When a molecule is undergoing chemical exchange,  $R_2$  has contributions from  $R_{ex}$ .  $R_2$  is a particularly useful measure of local

dynamics because it is the only rate among the three that depends on the spectra density at zero frequency  $J(0)$ . Hence it is useful to have measures which contain contributions from  $J(0)$  which are not affected by chemical exchange. There are no contributions to the other two measures  $R_1$  and NOE from exchange and the experimental measures are just average values over the major and minor states. So they largely report on the major state. Hence a new approach is required only for  $R_2$ . Two different experiments are discussed [Kroenke et al., 1998, Hansen et al., 2007], both of which use linear combinations of rates related to  $R_2$  to cancel the effects of exchange.

## 7.1 $^1\text{H}$ - $^{15}\text{N}$ Dipole-CSA cross-correlated measurement as a means of measuring the ground state $J(0)$

The  $^{15}\text{N}$  transverse relaxation rate depends on the spin state ( $\alpha$  or  $\beta$ ) of the amide proton due to dipole-CSA cross-correlated relaxation effects. In the TROSY experiment this effect is exploited to record spectra of large molecules. The dipole-CSA cross-correlated relaxation rate can be used to obtain information regarding  $J(0)$  [Kroenke et al., 1998, Tjandra et al., 1996]. This can be understood easily:

$$\begin{aligned} R_{2,Trosy} &= R_2 - \eta_{xy} + R_{ex} \\ R_{2,AntiTrosy} &= R_2 + \eta_{xy} + R_{ex} \end{aligned} \tag{34}$$

Here  $R_{2,Trosy}$  and  $R_{2,AntiTrosy}$  are the relaxation rates of the Trosy and AntiTrosy components and  $\eta_{xy}$  is transverse cross-correlated relaxation rate.  $R_{ex}$  is the same for both the components as it depends on  $\Delta\omega$ ,  $p_b$ ,  $k_{ex}$  which are the same for both the components. So we have:

$$\eta_{xy} = \frac{R_{2,AntiTrosy} - R_{2,Trosy}}{2} \tag{35}$$

with

$$\eta_{xy} = \frac{\sqrt{3}}{6} cdP_2(\cos \beta)[4J(0) + 3J(\omega_N)] \quad (36)$$

Hence  $\eta_{xy}$  provides a measure of  $J(0)$  that is not affected by chemical exchange. Here  $\beta$  is the angle between the principle axis of the CSA tensor and the N-H bond vector. Pulse sequences to measure  $\eta_{xy}$  [Tjandra et al., 1996] and the utility of  $\eta_z$  can be found in [Kroenke et al., 1998].

## 7.2 Linear combinations of $^1\text{H}$ and $^{15}\text{N}$ SQ and MQ relaxation rates to measure ground state $J(0)$

In the approach of Hansen, Yang, Feng, Zhou, Wiesner, Bai, and Kay [Hansen et al., 2007] a linear combination of SQ and MQ relaxation rates,  $R_\Sigma$  is used.

$$R_\Sigma = \frac{1}{2} [R_2(2H_xN_z) + R_2(2H_zN_x) - R_2(2H_xN_x) - R_1(2H_zN_z)] \quad (37)$$

we can rewrite this as

$$R_\Sigma = R_{dd} + \Delta R_{ex} \quad (38)$$

with

$$R_{dd} = \frac{d_{HN}^2}{8} \left[ 4J(0) + \frac{1}{2}J(\omega_H - \omega_N) - 3J(\omega_N) - 3J(\omega_H) + 3J(\omega_H + \omega_N) \right] \quad (39)$$

and

$$\Delta R_{ex} = \frac{1}{2} [R_{ex}(H_x) + R_{ex}(N_x) - R_{ex}(2H_xN_x)] \quad (40)$$

Now in the limit of slow exchange  $\Delta R_{ex} = 0.5[k_1 + k_1 - k_1] \neq 0$ . However in the limit of fast exchange (if ZQ and DQ are interchanged during the measurement of  $R(2H_xN_x)$ )  $\Delta R_{ex} = 0$ . By applying strong spin locks during the measurement of  $R(2H_xN_z)$ ,  $R(2H_zN_x)$  and  $R(2H_xN_x)$  (figure 14) the slow and intermediate timescale exchange can be quenched. This

leaves only fast timescale exchange which cancels to make  $R_\Sigma$  exchange free with  $R_\Sigma = R_{dd}$ .  $R_{dd}$  depends only the N-H dipole-dipole interaction and does not have any CSA contributions. This is a subtle advantage of this method as the CSA tensor varies (by about 10%) from site to site in the molecule and is usually not determined in a sitespecific manner. However the N-H bond length which affects the dipolar interaction between  $^{15}\text{N}$  and  $^1\text{H}$  is relatively invariant for the various amide groups in the backbones of proteins. This experiment has been used to study the local motion in a stabilized folding intermediate of apocytochrome  $b_{562}$  which shows severe line broadening due to exchange (figure 15).

### Problems

1. What is the effect of exchange on the  $S^2$  (order parameter square) and  $\tau_c$  (rotational correlation time) values extracted from  $R_2$  data that has  $R_{ex}$  contributions?
2. Confirm that  $R_{ex}$  is the same for the Trosy and Anti-Trosy components in equation (34). Do this by drawing a schematic spectrum of the ground and excited state spectra without decoupling.
3. Verify that  $\Delta R_{ex}$  in equation (40) reduces to zero in the case of fast exchange. Use the expressions for fast exchange given in equation (33).

## 8 References

A. D. Bain. Chemical exchange in NMR. *Prog Nucl Mag Reson Spectrosc*, 43:63–103, 2003.

John Cavanagh, Wayne J Fairbrother, Arthur G Palmer, Nicholas J Skelton, and Mark Rance. *Protein NMR Spectroscopy: Principles and Practice*. Academic Press, second edition, 2006.

N A Farrow, O Zhang, J D Forman-Kay, and L E Kay. A heteronuclear correlation exper-

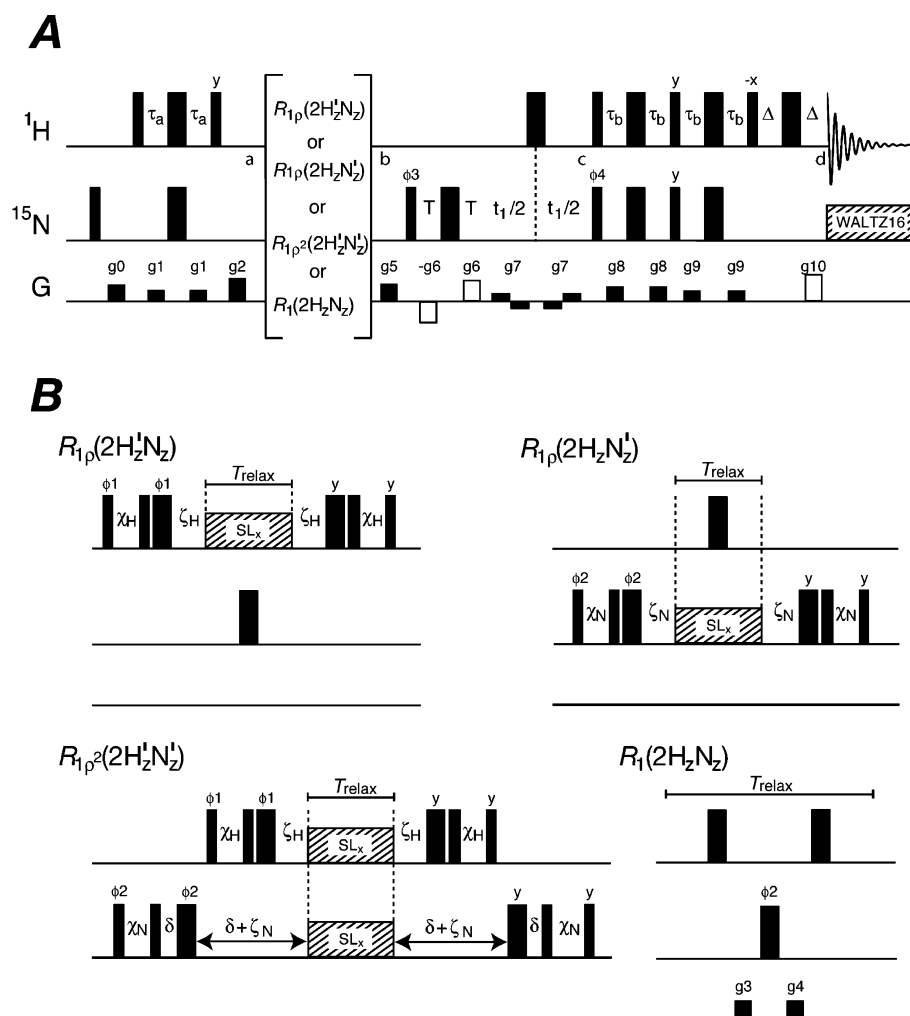


**Figure 14:** Pulse sequences to measure  $R(2H_zN_z)$  and  $R(2H_xN_z)$ ,  $R(2H_zN_x)$ ,  $R(2H_xN_x)$  under strong spinlock. See [Hansen et al., 2007] for details.

iment for simultaneous determination of  $^{15}\text{N}$  longitudinal decay and chemical exchange rates of systems in slow equilibrium. *J Biomol NMR*, 4(5):727–734, 1994.

DF Hansen, D Yang, H Feng, Z Zhou, S Wiesner, Y Bai, and LE Kay. An exchange-free measure of  $^{15}\text{N}$  transverse relaxation: an nmr spectroscopy application to the study of a folding intermediate with pervasive chemical exchange. *J Am Chem Soc*, 129(37):11468–11479, 2007.

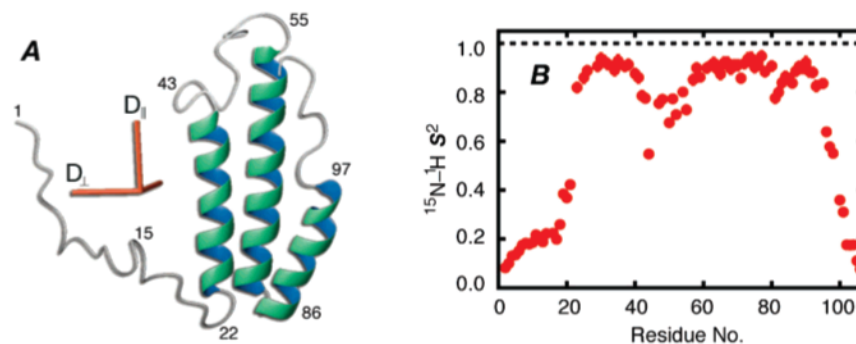


**Figure 15:** Pico-nanosecond dynamics in the stabilized folding intermediate of apocytochrome  $b_{562}$  studied using the pulse sequences described in figure 14. In spite of large  $R_{ex}$  contributions ps-ns motion can be studied. It is clear that the N and C terminus are very flexible and the first and last helix are not formed in solution. See [Hansen et al., 2007] for details.

DF Hansen, P Vallurupalli, and LE Kay. An improved  $^{15}\text{N}$  relaxation dispersion experiment for the measurement of millisecond time-scale dynamics in proteins. *J Phys Chem B*, 112(19):5898–5904, 2008.

D. L. Hasha, T. Eguchi, and J. Jonas. High-pressure NMR-study of dynamical effects on conformational isomerization of cyclohexane. *J Am Chem Soc*, 104(8):2290–2296, 1982.

DM Korzhnev, VY Orekhov, and LE Kay. Off-resonance  $r(1\rho)$  NMR studies of exchange dynamics in proteins with low spin-lock fields: an application to a fyn sh3 domain. *J Am Chem Soc*, 127(2):713–721, 2005.

CD Kroenke, JP Loria, LK Lee, M Rance, and AG Palmer. Longitudinal and transverse  $\text{H1-N15}$  dipolar  $\text{N15}$  chemical shift anisotropy relaxation interference: Unambiguous determination of rotational diffusion tensors and chemical exchange effects in biological macromolecules. *J Am Chem Soc*, 120(31):7905–7915, 1998.

J P Loria, M Rance, and A G 3rd Palmer. A TROSY CPMG sequence for characterizing chemical exchange in large proteins. *J Biomol NMR*, 15(2):151–155, 1999.

- P Lundstrom and M Akke. Off-resonance rotating-frame amide proton spin relaxation experiments measuring microsecond chemical exchange in proteins. *J Biomol NMR*, 32(2): 163–173, 2005.
- A G 3rd Palmer, C D Kroenke, and J P Loria. Nuclear magnetic resonance methods for quantifying microsecond-to-millisecond motions in biological macromolecules. *Methods Enzymol*, 339:204–238, 2001.
- N Tjandra, A Szabo, and A Bax. Protein backbone dynamics and n-15 chemical shift anisotropy from quantitative measurement of relaxation interference effects. *J Am Chem Soc*, 118:6986–6991, 1996.